nature portfolio

https://doi.org/10.1038/s41587-021-00897-5

Supplementary information

Long-term wireless streaming of neural recordings for circuit discovery and adaptive stimulation in individuals with Parkinson's disease

In the format provided by the authors and unedited

Supplemental methods

Further details on surgical lead placement. The paddle lead was placed in the subdural space through the same frontal burr hole used for the subthalamic lead. At least one contact covered the posterior precentral gyrus (presumed primary motor cortex), approximately 3 cm from the midline on the medial aspect of the hand knob. Adequate localization of the cortical contact array was confirmed using intraoperative CT computationally merged to the patient's preoperative MRI[1] (Stealth8 Cranial software, Medtronic Inc.) Functional localization of the cortical contact array was verified by reversal of the N20 somatosensory-evoked potential from median nerve stimulation (**Figure 2b**). The exiting wire from the cortical contact array was secured to the skull with a titanium miniplate. The subthalamic lead was placed using frame-based stereotaxy and confirmed by microelectrode recording in the awake state using standard methods[2]. Proper location in the motor territory of the STN was verified by eliciting movement-related single-cell discharge patterns. The DBS lead was placed with the middle two contacts in dorsal (motor) STN, the most superior contact dorsal to the STN, and the most inferior contact in ventral STN (**Figure 2a**). The free ends of the cortical and subthalamic leads were coiled under the ipsilateral parietal scalp. The remaining hardware was placed under general anesthesia. The free ends of the cortical and subthalamic leads were connected to the lead extenders, which were tunneled down the neck to the IPG. Each IPG was connected to the ipsilateral cortical and STN leads. Medical adhesive was placed at the junction of the lead extenders and IPG to reduce contamination of neural signals by EKG artifacts.

*Details for analysis of in-clinic data in defined on and off states (**Extended Data Figure 3**).* Data were inspected for artifacts and contiguous 30s data segments for which no packet loss occurred were chosen for analysis. We calculated power spectral density (PSD) using the Welch Method in Matlab (pwelch, 500 ms window, 250 ms overlap) from 4 contact pairs (0-2, 1-3 in STN and 8-10, 9-11 in the cortical lead) per implant side. This yielded 8 PSD's per patient in the on and off medication condition. For each PSD we computed the average beta signal (13-30 Hz) subcortically or gamma (65-85 Hz) cortically across patients. We compared the average frequency-specific spectral power on/off medication response using generalized estimating equations (GEE) to account for non-independence of recording locations within patients[3] using the GEEQ toolbox for Matlab. Resulting p-values were corrected for multiple comparisons using a Bonferroni correction. For movement-related changes in spectral power, data were filtered using a two way 3rd order FIR filter (eegfilt from eeglab toolbox with fir1 parameters) and

bandpassed in frequencies between 1-200 Hz. Data from all trials were aligned relative to the onset of movement and averaged. The averaged amplitude was normalized by a 1000 ms window prior to cue presentation (time 0). Data were z-scored by subtracting the average baseline amplitude and dividing by the baseline standard deviation. This z-score procedure was performed for each frequency separately.

Further details on home data collection: Maintaining continuity of data streaming. Benchtop tests showed that streaming four time domain channels at 500Hz while providing therapeutic stimulation can be done for approximately 30 hr before recharging the RC+S pulse generator. However, several factors may reduce the duration of continuous streaming. The CTM (clinician telemetry module) relay device (**Figure 1**), as supplied by the manufacturer, is powered by two AAA batteries that only last for 4-5 hr during streaming. We therefore developed an external "battery pack" for the CTM that extends this range to 12 hr. Both RC+S pulse generators can be recharged simultaneously in 30 minutes. For most home streaming we used lower sampling rates (250 Hz) than the device allows, in order to cap the bitrate at 4500 bits/s and allow for longer range and fewer dropped packets. Our patients wore a specialized vest with pockets for the CTM so that it remained in close proximity to the DBS device to avoid frequent packet drops.

Neural data collection and processing for motor task at home. Patients also performed a movement task similar to the in-clinic iPad task but optimized for working in a web browser with low powered computers using the jsPsych package[4]. Patients performed 60 single arm reaches to a target presented in one of four locations on the screen following a cue to move with either the left or the right hand, and on/off therapeutic stimulation (**Supplemental Figure 1**). The full code for the task as well as a version which runs on any web browser can be found here: https://roeegilron.github.io/sampleMovementTask/index.html. Of note this task was run entirely remotely without the physical presence of the research staff. Synchronization of neural data and task data was done using the clock of the patients' study computer. Two channels were recorded from motor cortex with a 1000 Hz sampling rate and data were analyzed using the same procedure described above in the "in-clinic" section.

Rationale for within-subjects modelling and avoidance of overfitting. Within-subjects modelling was statistically robust due to the availability of hundreds of thousands of data segments (input), for each subject, each associated with a particular motor state (supervised labels - derived from a wearable monitor). Development of between-subject models would have required many more subjects, and would be less accurate at the individual subject level due to inter-individual

variability in motor signs that is characteristic of PD. Several factors in our analysis were used to assess and guard against potential overfitting of the LD classifier. First, we did not use any hyperparameter or feature selection procedure in our cross validation. Feature selection is shown to produce overfitting even in the presence of cross validation[5]. Second, the ratio of the number of data segments to model features (spectral density and coherence measures) was large (at least 100x), and two of the LDA models tested only use a single feature while the maximum number of features tested was 16. Third, we are using a linear model (LDA), that is unlikely to overfit with such a small feature set compared to deep learning or models that are polynomial in nature. Finally, we test each model against a non-parametric null distribution created using shuffled PKG labels. This tests the null hypothesis that "random" data with the same covariance structure overfits the data using the same procedure. By only considering statistically significant results, this greatly increases our confidence in the ability of our model to classify out-of-sample examples.

Details of adaptive DBS Settings for STN beta band controller (RCS03). Stimulation parameters were: stimulation rate 158.7Hz, pulse width 60 μs, with monopolar stimulation (2+C-). Upper and lower amplitude limits were 1.4 mA and 0 mA, chosen based on the patients' historical self selected limits, when allowed to adjust amplitude with the patient programmer during an earlier period of standard open loop DBS. Sensing was configured in "sandwiched" configuration (sensing from contacts 1 and 3, on either side of the monopolar stimulating contact) to provide common mode rejection of stimulation artifact. The power bands for sensing were set at between 17.09-19.04 Hz, surrounding this subject's beta peak. When the STN beta control signal exceeded the upper threshold, the stimulation was increased and when it dropped below the lower threshold, stimulation was decreased. Sense blanking was 0.555 ms. Both the ramp up and ramp down rate was 0.01 mA.

Details of adaptive DBS settings for cortical gamma band controller (RCS01). Stimulation parameters were: 130.2 Hz, pulse width 60 μs, with monopolar stimulation (1+C-). Stimulation amplitude limits were 2.6 mA and 3.4 mA, selected so as to provide more stimulation in off periods, and slightly less in on periods, compared to his open loop setting of 2.7 mA. Cortical sensing contacts were +9-11 and the pre-configured power band was set between 62.99-66.89 Hz to surround this subject's gamma peak. When the cortical gamma control signal exceeded the upper threshold, the stimulation was decreased; and when it dropped below the lower threshold, stimulation was increased. Sense blanking was set at 1.05ms. Of note the ramp up rate was set at 0.01 mA/s and the ramp down rate at 0.07 mA/s, such that in the presence of

elevated cortical gamma stimulation was ramped down much faster than it was ramped up. This was to prevent or rapidly abort dyskinesias.

Algorithm risk management for adaptive DBS. Testing adaptive DBS at home requires adherence to design controls (FDA 820.30) to ensure that design requirement are met and that stimulation is delivered safely[6]. In addition to the risk analysis required in the IDE (investigational device exemption) for this study, we conducted a more detailed risk analysis (as mandated by FDA 820.3). To mitigate the main risk, that of excessive or inadequate stimulation, two strategies were used: first, a clinician verified that the selected upper and lower stimulation limits were safe and tolerable to patients. These limits were set on the clinician programmer, and could not be exceeded during adaptive control. Second, patients were instructed to return to their open loop settings using their patient controller if they experienced any adverse symptoms from adaptive DBS.

Supplemental results

Details of In-clinic brief recordings and effects of levodopa in defined on and of states

Data were streamed in clinic three weeks after implantation in order to verify recording quality, the presence of movement related activity, and the effects of levodopa in defined on/off states. Example time series data from one hemisphere are in **Extended Data Figure 3a**. In the sensorimotor cortex, initiation of movement was associated with canonical movement-related reduction in beta band activity, with a concomitant increase in broadband 50-200 Hz activity, reflecting local cortical activation[7] (**Extended Data Figure 3b).** Previous perioperative recordings in humans using externalized brain leads have shown that antiparkinsonian dopaminergic medications such as levodopa reduce the amplitude of beta band (13-30 Hz) oscillations in the basal ganglia[8]. To confirm that this effect is also observed in recordings streamed from the implanted neural interface, we evaluated resting state power spectral density in defined medication states: after 12 hr withdrawal of antiparkinsonian medications (“off”) and after a therapeutic dose of levodopa/carbidopa (“on”). **Extended Data Figure 3c** shows a single-subject example with reduction in STN beta band oscillations in the on-medication state as well as emergence of a narrowband gamma oscillation at 80 Hz. Averaging power spectra across all subjects (**Extended Data Figure 3D**) showed that the on-medication state was associated with the expected reduction in beta band oscillations in the STN ($p < 0.001$,

Generalized Estimating Equations (GEE)). Motor cortex changes were not significant across the group, which may reflect inter-subject variability in the expression of cortical biomarkers, or the difficulty of capturing more subtle biomarkers in brief recordings.

In-clinic versus at home recordings

In general, in-clinic recordings are analyzed by pooling brief "snapshots" of each subjects' neural data across all subjects. Long-term recording at home, in contrast, can be performed over prolonged periods that capture ongoing fluctuations in disease signs and symptoms in individuals. This allows the use of within-subjects statistics, facilitating the identification of *personalized* biomarkers that may be specific to that subjects' unique disease profile. Comparison between in-clinic and home recordings shows that for some subjects home recordings may broadly recapitulate oscillatory phenomena discerned in defined on/off states in-clinic (compare **Extended Data Figure 3c** and **Figure 3c)**. However, especially in patients with milder fluctuations, home recordings and within-subject statistics can detect oscillatory phenomena that are more subtle or more individualized. For example, in one subject (RCS04), subthalamic gamma oscillations and STN-cortex gamma coherence were prominent in at-home recordings in the mobile state but were not detected in brief in-clinic recording (**Supplemental Figure 1**).

Broadband cortical responses detectable in the presence of therapeutic stimulation

The capacity for sampling rates up to 1000 Hz and favorable signal to noise ratio for high frequencies allows novel types of neuroscience studies utilizing "high gamma" responses, which has been problematic with early devices[9]. High gamma" also referred to as "broadband" or "broadband gamma" reflects localized cortical function[7, 10] and is a non-oscillatory phenomenon that is thought to reflect underlying asynchronous spiking. These broadband responses are distinct from narrowband gamma oscillations in the 60-90 Hz range and have previously been studied almost exclusively using externalized leads[7, 11]. Here, we demonstrate canonical movement motor cortex broadband changes, time locked to an arm movement in all five subjects, in the presence and absence of therapeutic stimulation (**Supplemental Figure 2**). Further, these task-related signal changes were collected from patients in their homes, with investigators participating remotely. This device capability opens new avenues for the study of localized cortical function at high spatial and temporal resolution, within defined tasks or during

normal activities, which can now be done in the home environment while investigators monitor remotely.

Unsupervised clustering of neural data for identification of distinct behavioral states.

The analysis of large amounts of neural data "supervised" by wearable monitors is labor-intensive and depends on the accuracy of the wearable monitor as well as a prospective understanding of the behavioral states that need to be tracked. Unsupervised clustering, in contrast, may provide efficient identification of individualized neural signatures of disease state from large data sets. This approach does not depend on patient compliance with a wearable monitor, patient reporting or clinician ratings and may identify previously unrecognized patterns of neural activity to generate new hypotheses about circuit mechanisms and biomarkers. We employed an unsupervised clustering method based on density of data points in dimensionality-reduced power spectra[12] (**Extended Data Figure 5**). This "density-based clustering" does not require defining the number of states (unlike k-means clustering). A second clustering method utilized power spectra of the brief in-clinic recordings done in defined behavioral states, as "templates" for unsupervised clustering in home data (**Extended Data Figure 5b**). Both methods identified clusters that broadly corresponded to PKG based state labels (**Extended Data Figure 5c**). The mean concordance was 74% (range 59%-89%) for density based clustering and 74.5% (range 59%-90%) for template based clustering (**Extended Data Figure 5c**). For subject RCS04, clusters were most evident for STN.

Thus, unsupervised clustering was able to distinguish brain states corresponding to on- and off-periods, similar to those identified with wearable monitors (**Extended Data Figure 5).** This method might also facilitate the identification of neural correlates of psychiatric states, for which objective tracking of symptoms severity at home is currently challenging[13]. Additionally, in disorders for which behavioral states are readily induced in-clinic by "provocative tests"[14], template-based clustering method (using the in-clinic data as templates) may allow identification of those states in home recordings.

Supplemental data illustrating efficacy of adaptive DBS at home

The **supplemental video** taken on two consecutive days shows that, during a time of day when the subject typically is bradykinetic (morning prior to taking first medications), adaptive control improved hand bradykinesia, by allowing a higher stimulation amplitude during that part of the medication cycle, compared to standard DBS. During a time of day when the subject is typically dyskinetic (afternoon) on standard DBS, adaptive DBS avoided dyskinesia by lowering stimulation amplitude at that time. For RCS03, the subject was unable to tolerate open loop DBS without self-adjusting stimulation amplitudes to 0 mA during periods of dyskinesia. Adaptive DBS allowed this subject to tolerate stimulation therapy without having to self-adjust levels throughout the day, by doing this adjustment automatically based on STN beta amplitude (**Figure 6a**). Both subjects had adaptive DBS testing *after* a period of clinically optimized open loop DBS, and both preferred adaptive stimulation as shown by their Patient Global Impression of Change (PGIC) ratings. RCS03 scored 7 ("A great deal better and considerable improvement," and RCS01 scored 6 ("better and a definite improvement").

Further detail on sensing during stimulation

When bidirectional interfaces are used for sensing *during* stimulation, the stimulation artifact can obscure low-amplitude signals. This has typically precluded detection of high frequency cortical broadband activity or sensing of any subcortical signals during stimulation from the same lead array[15]. Using a computer-based movement task implemented at home, we demonstrate cortical movement-related broadband or "high gamma" changes both in the presence and in the absence of therapeutic STN DBS (**Supplemental Figure 2**). We also successfully evaluated STN activity during therapeutic stimulation from an adjacent contact on the same array, by using a "sandwiched" sensing configuration to take advantage of common mode rejection (bipolar sensing from the contacts on either side of a monopolar stimulating contact). We show that chronic therapeutic stimulation reduces STN beta power during normal home activities (**Extended Data Figure 7a**), whereas prior studies have only evaluated the effect of DBS on STN physiology in clinic in the absence of voluntary movement[16, 17]. Both type of sensing have previously only been possible using externalized leads[7, 11, 16, 17] or by sensing from an implanted device in a "distributed mode" in which signals are processed within an external computer[15].

In three subjects, we examined effects of standard open-loop therapeutic stimulation, over many hours of recording, on the distribution of beta band activity. Sensing was done *after* clinical optimization of therapeutic DBS (1–5 months after initiating DBS) and compared to the neural

activity in the 2-4 weeks post-implantation prior to initiating DBS. Violin plots show how chronic stimulation affects the variability of STN beta band activity (**Extended Data Figure 7b**). Prior to therapeutic stimulation, the range of beta amplitudes showed a bimodal distribution, likely corresponding to on- and off-states. Open loop therapeutic DBS reduced the median beta activity. In two subjects, open loop DBS also collapsed the bimodal distribution of beta activity into a unimodal one, presumably reflecting amelioration of motor fluctuations, while in the other, open loop DBS only lowered the median beta but preserved a bimodal distribution. This finding has translational potential for selecting patients who could benefit from adaptive DBS. When standard open loop DBS fails to collapse the bimodal distribution of a neural biomarker, that patient may stand to gain additional benefit from adaptive DBS, to more effectively shape the distribution of the relevant biomarker by selectively reducing it only when it is elevated above physiological levels.

Supplementary Table 1. Lead locations from fusion of postoperative CT to preoperative MRI

Subject	AC-PC coordinates of DBS lead tip in mm: left*	AC-PC coordinates of DBS lead tip in mm: right*	Lateral and AP coordinates of lead at dorsal STN in mm: left **	Lateral and AP coordinates of lead at dorsal STN in mm: right**	Sagittal plane approach angle (degrees from horizontal)	Coronal plane approach angle (degrees from vertical)	Cortical array laterality (mm) at central sulcus: left	Cortical array laterality (mm) at central sulcus: right
RCS01	-9.8, -3.3, -6.5	9.1, -2.5, -6.9	-10.1, -2.4	10.2, -1.1	Left: 60.7 Right:67.1	Left:-14.6 Right:20.0	29.0 (contact 1)	24.8 (contact 1)
RCS02	-11.8, -3.4, -5.8	9.1, -4.0, -5.6	-11.4, -2.7	10.9,-3.2	Left: 51.4 Right: 52.9	Left: -17 Right: 8.7	21.1 (contact 1)	28.9 (contact 1)
RCS03	-10.2, -3.9, -7.0	9.4, -1.4, -6.6	-10.9, -3.2	10.4, -0.2	Left:70.6 Right: 61.6	Left: 16.6 Right: 21.6	25.4 (contact 2)	29.3 (contact 2)
RCS04	-10.5, -3.0, -6.8	9.4, -1.1, -7.8	-11.3, -1.5	10.2, 0	Left: 64.8 Right:66.5	Left:16.7 Right:14.4	33.1 (contact 1)	22.3 (contact 1)
RCS05	-8.5, -1.1, -7.0	12.2, -1.2, -6.5	-10.1, 0.1	12.9, 0.4	Left: 69.3 Right: 65.1	Left: 22.8 Right: 20.9	29.8 (contact 1)	35.5 (contact 1)

*coordinates are lateral, anteroposterior, and vertical with respect to midpoint of line connecting the anterior (AC) and posterior commissures (PC)

** coordinates are lateral and anteroposterior, in the axial plane 4 mm inferior to the line connecting anterior and posterior commissures

References

1. Shahlaie, K., Larson, P.S. & Starr, P.A. Intraoperative computed tomography for deep brain stimulation surgery: technique and accuracy assessment. *Neurosurgery* **68**, 114-124; discussion 124 (2011).
2. Starr, P.A. Placement of deep brain stimulators into the subthalamic nucleus or Globus pallidus internus: technical approach. *Stereotactic and functional neurosurgery* **79**, 118-145 (2002).
3. Shimamoto, S.A. et al. Subthalamic nucleus neurons are synchronized to primary motor cortex local field potentials in Parkinson's disease. *J Neurosci* **33**, 7220-7233 (2013).
4. de Leeuw, J.R. jsPsych: a JavaScript library for creating behavioral experiments in a Web browser. *Behavior research methods* **47**, 1-12 (2015).
5. Smialowski, P., Frishman, D. & Kramer, S. Pitfalls of supervised feature selection. *Bioinformatics* **26**, 440-443 (2010).
6. Gunduz, A. et al. Adding Wisdom to “Smart” Bioelectronic Systems: A Design Framework for Physiologic Control including Practical Examples. *Bioelectronics in Medicine* **2** (2019).
7. Crone, N.E., Miglioretti, D.L., Gordon, B. & Lesser, R.P. Functional mapping of human sensorimotor cortex with electrocorticographic spectral analysis. II. Event-related synchronization in the gamma band. *Brain* **121 (Pt 12)**, 2301-2315 (1998).
8. Brittain, J.S. & Brown, P. Oscillations and the basal ganglia: motor control and beyond. *NeuroImage* **85 Pt 2**, 637-647 (2014).
9. Swann, N.C. et al. Chronic multisite brain recordings from a totally implantable bidirectional neural interface: experience in 5 patients with Parkinson's disease. *Journal of neurosurgery* **128**, 605-616 (2018).
10. Voytek, B. & Knight, R.T. Dynamic network communication as a unifying neural basis for cognition, development, aging, and disease. *Biological psychiatry* **77**, 1089-1097 (2015).
11. Miller, K.J. et al. Spectral changes in cortical surface potentials during motor movement. *J Neurosci* **27**, 2424-2432 (2007).
12. Rodriguez, A. & Laio, A. Machine learning. Clustering by fast search and find of density peaks. *Science (New York, N.Y* **344**, 1492-1496 (2014).
13. Jiang, Z. et al. Classifying Major Depressive Disorder and Response to Deep Brain Stimulation Over Time by Analyzing Facial Expressions. *IEEE transactions on bio-medical engineering* **PP** (2020).
14. Brooks, H. et al. Developing image sets for inducing obsessive-compulsive checking symptoms. *Psychiatry research* **265**, 249-255 (2018).
15. Velisar, A. et al. Dual threshold neural closed loop deep brain stimulation in Parkinson disease patients. *Brain stimulation* **12**, 868-876 (2019).
16. Tinkhauser, G. et al. The modulatory effect of adaptive deep brain stimulation on beta bursts in Parkinson's disease. *Brain* **140**, 1053-1067 (2017).
17. Kuhn, A.A. et al. High-frequency stimulation of the subthalamic nucleus suppresses oscillatory beta activity in patients with Parkinson's disease in parallel with improvement in motor performance. *J Neurosci* **28**, 6165-6173 (2008).

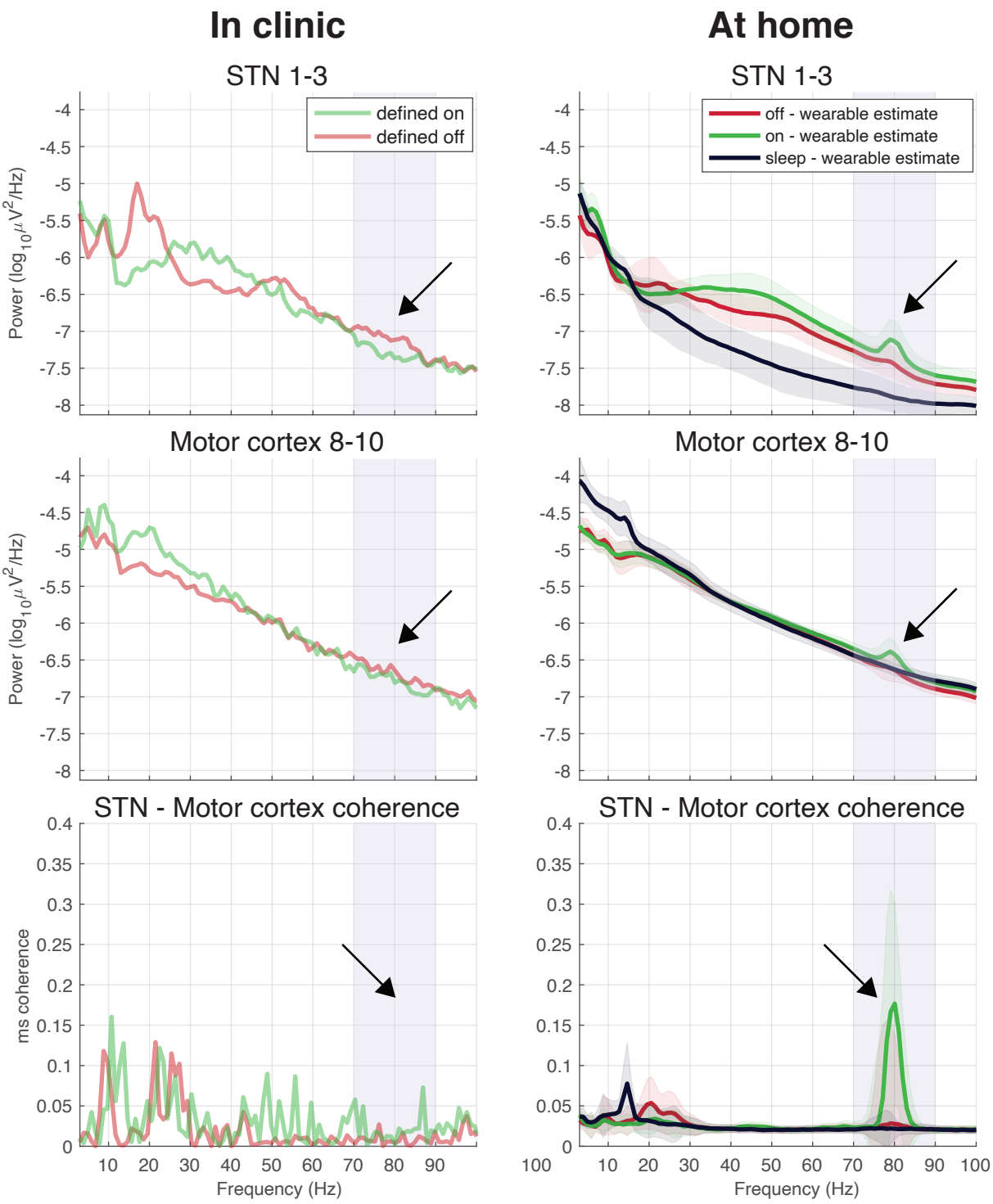

Supplemental Figure 1 - Example comparison of neural biomarkers collected in-clinic at rest in defined on/off states (for 30 seconds, left column), versus at-home during normal activities (for > 100 hours, right column). Data are from RCS04. Top row, STN subcortical contact +1-3; middle row, Motor cortex 8-10; lower row, coherence between STN and motor cortex. Note that narrowband gamma oscillations at 80 Hz in the on-state (black arrows) are not detected in the brief in-clinic recordings, but are apparent in home recordings. In home recording (right column) solid line represents mean activity per condition with shading indicating standard error of the mean. Shading represents one standard deviation (at home data, right column). Of note, sleep (black lines) abolishes the gamma band biomarker (see also **Extended Data Figure. 6**).

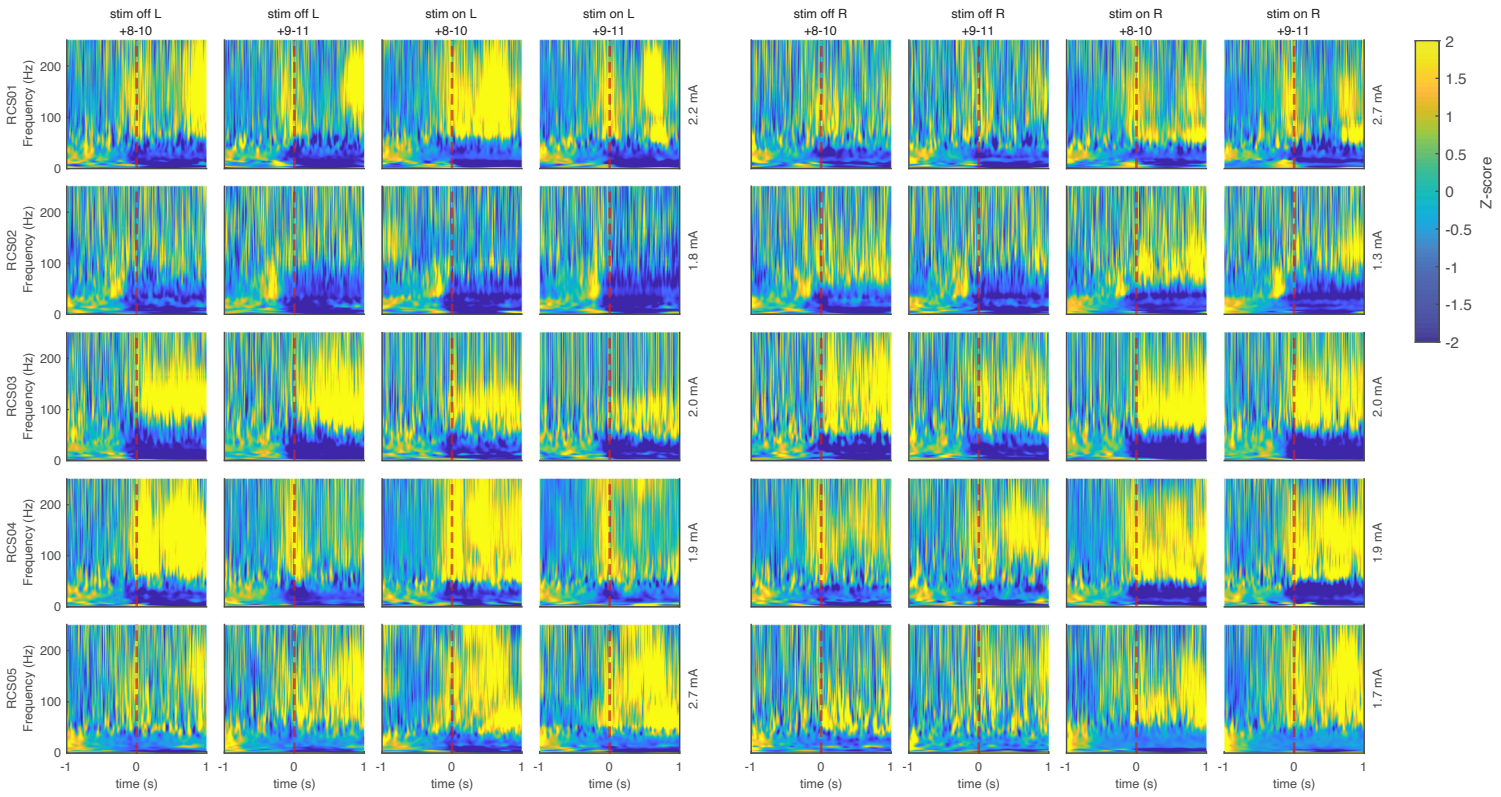

Supplemental Figure 2. Canonical movement related broadband gamma increases are detected with and without chronic therapeutic neurostimulation. Spectrograms of field potential activity for both cortical contacts pairs (+8-10, +9-11), both hemispheres, on and off of therapeutic stimulation, for all subjects. Recordings took place at least 6 months post implant (range 184-451 days) on the patient's home computer with research staff supervising the task remotely, and without any external synchronization pulses. Patient conducted 60 reaches to one of four targets placed on the screen after a fixation (no target present) and "hold" period (target appears but cue for movement not given). Dotted red dashed line are represent the cue to move. Data from each subject are in separate rows. The four left subplot columns were recorded from L motor cortex with reaches conducted by contralateral hand (R). The four right subplot columns were recorded from R motor cortex with movement from contralateral hand (L). Column headings indicate the presence or absence of stimulation. Ipsilateral subcortical stimulation levels for each hemisphere are listed on the 4th and 8th column from the left. All subjects show canonical movement related beta decreases (8-35Hz) and gamma broadband increases (50-200 Hz). Color scale is z-score, data were sampled from the two motor cortex channels simultaneously at a sampling rate of 1000 Hz.